Pergamon

Int. J. Heat Mass Transfer. Vol. 40, No. 12, pp. 2941–2947, 1997

Printed in Great Britain
0017–9310/97 $17.00 + 0.00

PII: S0017–9310(96)00337–7

Interferometric study of interaction of free convection with surface radiation in an L corner

V. RAMMOHAN RAO, C. BALAJI† and S. P. VENKATESHAN‡

Heat Transfer and Thermal Power Laboratory, Department of Mechanical Engineering, Indian Institute of Technology, Madras 600 036, India

(*Received* 20 *October* 1995 *and in final form* 6 *September* 1996)

Abstract—A detailed experimental investigation of interaction of free convection and radiation in a single fin mounted on a heated horizontal base has been carried out. The study makes use of a differential interferometer for estimating the convective heat fluxes. A numerical method coupled with the experimentally measured convective fluxes is used to evaluate the radiative fluxes. Experiments were conducted to study the effect of fin height, surface emissivity and the base temperature level on convection and radiation. Based on the experiments correlations have been presented for both the total and radiative heat transfer rates from the fin flats. Comparisons are made between the experimental results and two-dimensional numerical computations based on finite volume method. © 1997 Elsevier Science Ltd.

1. INTRODUCTION

Natural convection heat transfer has been receiving much attention in recent times because of many applications it has in diverse areas. Typical applications include insulation design, cooling of electronic equipment, solar thermal systems, etc. Natural convection heat transfer provides a noiseless method of thermal control without any expenditure of high grade energy. In the case of cooling of electronic equipment the geometries used fall into the category of channels, L shaped corners, vertical and horizontal fin arrays. In most of these applications the temperature levels are limited to a range from room temperature to about 100°C. In this temperature range surface radiation and free convection are equally important. Even then there have not been many studies reported in the literature that consider the interaction between these two modes of heat transfer. The present study is an experimental investigation of heat transfer by free convection and radiation from a single vertical fin mounted on a heated horizontal base.

Literature pertinent to this geometry is limited to a few papers in the published literature. The earliest work in this genre was the experimental study of a vertical corner by Van Leeuwan *et al.* [1]. Rodigheiro and de Socio [2] performed experiments with air for an L corner with an adiabatic horizontal leg (base) and an isothermal (heated) vertical leg (fin). The same geometry was recently studied numerically by Angirasa and Mahajan [3]. Ruiz and Sparrow [4] considered V-shaped and L-shaped corners losing heat to water, experimentally. The two legs of the corner were kept at the same uniform temperature. Correlations for calculating heat transfer from both the legs were provided. However, none of these considered the presence of radiation. Also, the boundary conditions do not reflect applications in a realistic way. Recently Balaji and Venkateshan [5] have presented a numerical study of an L corner that includes the interaction of free convection with radiation, by a finite volume method. They considered various types of boundary conditions on both the legs. Specifically, the vertical leg was non isothermal and its temperature variation in the height direction was found by a balance between thermal conduction in the material of the fin, surface radiation and free convection at the surface. Free convection flow was assumed to be two-dimensional. The present study is an experimental investigation of the same problem but without the two-dimensional restriction on the flow.

2. EXPERIMENTAL PROCEDURE

2.1. *Construction of the single fin assembly*

A schematic of the single fin assembly is shown in Fig. 1. The aluminum fin is fixed between two aluminum base blocks of size $50 \times 50 \times 10$ mm. Use of an aluminum base of high thermal conductivity helps in maintaining a uniform temperature throughout the base. The width of the fin assembly was fixed as 50 mm because of the restricted space available in the differential interferometer test section. Two 5 mm through holes were drilled along the length of the base. The fin flats were 10 mm longer than the exposed

† Present address: Department of Mechanical Engineering, Regional Engineering College, Tiruchirapalli 620 015, India.

‡ Author to whom correspondence should be addressed.

NOMENCLATURE

F_{i-j}	view factor between elements i and j (see Fig. 4)
g	acceleration due to gravity [m s^{-2}]
G	irradiation [W m^{-2}]
H	fin height [m]
K	differential interferometer constant [m^{-1} K^{-1}]
k	thermal conductivity [W m^{-1} · K^{-1}]
m	fringe shift factor, the ratio of fringe deflection to fringe spacing
Nu	Nusselt number based on height, $gH/[k_a(T_b - T_\infty)]$
N_{r-c}	radiation conduction interaction parameter $(2\sigma\varepsilon_f T_b^3 H^2)/(k_f t)$
N_{v-c}	convection conduction interaction parameter $(2Kk_a H^2 T_b)/(k_f t)$
Pr	Prandtl number, ν/α
q	heat flux [W m^{-2}]
Ra_H	Rayleigh number based on fin height, $g\beta(T_b - T_\infty)H^3/(\nu\alpha)$
T	temperature [K]
t	fin thickness [m]
x	distance along the surface [m]
y	distance normal to the surface [m].

Greek symbols

α	thermal diffusivity of air [m^2 s^{-1}]
β	volummetric expansion coefficient of air [K^{-1}]
Γ	nondimensional irradiation, $G/\sigma T_b^4$
ε	hemispherical emissivity
ν	kinematic viscosity of air [m^2 s^{-1}]
θ	non-dimensional temperature, T/T_b
ρ	density of air [kg m^{-3}]
σ	Stefan–Boltzmann constant [5.67 × 10^{-8} W m^{-2} · K^{-4}]
ξ	non-dimensional x coordinate.

Subscripts

a	pertaining to air
b	pertaining to the base
c	convective
f	pertaining to the fin flat
r	radiative
t	total
∞	ambient.

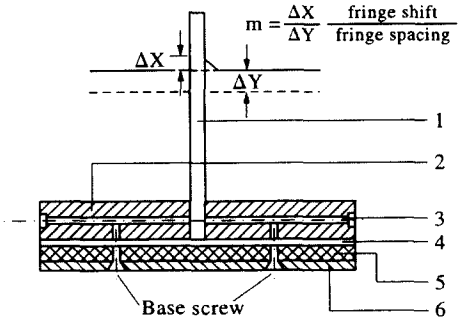

(1) Fin (2) Base blocks
(3) Tie bar (4) Electric heater
(5) Bottom plate (6) Insulation

Fig. 1. Constructional details of the single fin assembly.

heights of 30, 50 and 70 mm, respectively, the extra length being in contact with the base plates, which were made in two segments. The fins were made of 1.5 mm aluminum sheet stock and the edges were machined flat. Two 5 mm holes were drilled symmetrically on a line parallel to the bottom edge and 5 mm away from it to match the through holes in the base blocks. Two rods of 4.5 mm diameter passing through these holes hold the fin flat in a vertical orientation with respect to the horizontal base and provide and intimate contact over the 10 mm margin between the flat and the base segments. A flat element heater prepared by winding nichrome wire on to a mica sheet of slightly smaller size than the base plate, with a uniform pitch, was used to heat the fin base. The heater element was kept sandwiched between the base plate segments and a bottom support plate with the help of two screws, as shown in Fig. 1. Metal to metal contact at the base was avoided by placing a mica sheet between the heater and the base. The base was insulated on the bottom side to prevent heat transfer to a stand on which the fin assembly was mounted. A copper–constantan thermocouple was fixed to the base side of the fin to measure the base temperature. Another thermocouple of the same type was fixed at the tip of the fin to measure the tip temperature.

2.2. *Measurement using the differential interferometer*

Measurement procedure using the differential interferometer available in this laboratory has been discussed in detail in an earlier publication [6]. Also, given there are the details regarding the various settings on the instrument. The measurement procedure consists in photographing the fringe patterns in the steady state, for a given heat input to the base of the single fin assembly. Analysis of the data alone is explained in detail, in the next section.

3. ANALYSIS AND PRESENTATION OF DATA

A differential interferometer gives the convective heat flux normal to a surface if the local temperature and the fringe shift at the surface are known. The

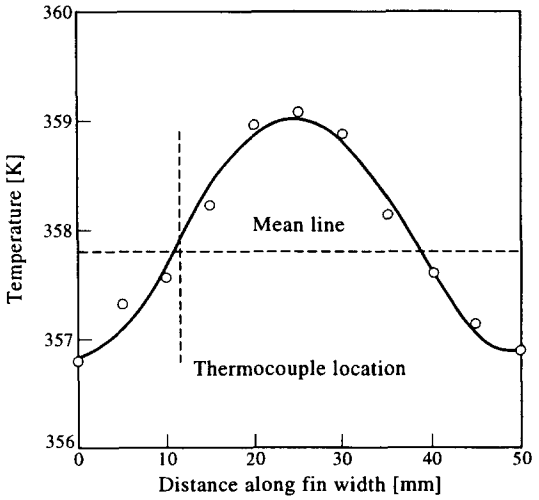

Fig. 2. Temperature variation along the width of the single fin at $x = H$ (tip). Location of a thermocouple that will indicate that average temperature is also indicated.

fringe shifts are due to the density differences in the fluid in a direction normal to the wall and these arise due to the temperature variations. These fringe shifts may be measured from an interferogram, but the measurement of local temperature is not easy since the temperature and the fringe shifts must be measured at the same location along the surface from which heat transfer is taking place. In order to circumvent this problem only the base and the tip temperatures are measured by thermocouples fixed at suitable locations as described later. These measured temperatures are used as boundary conditions in solving the fin equation. Since the fringe shift information yields only the convective fluxes, determination of the radiative fluxes needs a second procedure that uses the radiosity–irradiation formulation. Since this formulation involves the local temperatures and since the fin equation involves the irradiations the two are coupled and therefore need an iterative solution.

3.1. *Measurement of base and tip temperatures*

Two copper–constantan thermocouples were used to measure the tip and base temperatures. Since the base is made of 10 mm thick aluminum it does not really matter where the thermocouple is fixed for measuring the fin base temperature. The base temperature was found to vary by no more than ± 0.2 K from end to end. The tip temperature, on the other hand, varied by as much as ± 1 K from an average temperature that occurred invariably at 15 mm from either extremity. A typical temperature profile in the cross-wise direction shown in Fig. 2 supports this. The case under consideration in Fig. 2 is for $H = 70$ mm, $\varepsilon_f = 0.85$ and heat input of 12.5 W. In all the experiments the thermocouple measuring the tip temperature was fixed at a distance of 15 mm from the nearest end.

3.2. *Measurement of fringe shift*

A Pentax K 1000 camera with a zoom lens was used to photograph the fringe pattern through the eye piece of the differential interferometer. Monochrome 35 mm film was used in all the experiments. The fringe shifts were measured from projected images of linear magnification equal to 4.3. Since the flow exhibits symmetry about the fin it was sufficient to measure the fringe shifts on one side of the fin. The fringe shift factor m is obtained by dividing the measured fringe shift by the fringe spacing. The fringe spacing is fixed by the choice of the instrument settings [6, 7].

3.3. *The fin equation and the radiation formulation*

An important assumption made in the formulation of the fin equation is that the temperature variation is one-dimensional with the temperature varying only with height. This is reasonable in view of the low Biot number based on fin thickness. Also the experiments showed that the difference between base and tip temperatures could be about 10 K while the end to end variation in temperature is limited to ± 1.0 K. The fin equation is derived by making an energy balance for a fin element as given in ref. [7]. Referring to Fig. 3, such a heat balance leads to the following equation.

$$\frac{d^2T}{dx^2} + \frac{2Kk_a}{k_f t} mT^2 + \frac{2\varepsilon_f}{k_f t}[\sigma T^4 - G]. \qquad (1)$$

G here refers to the irradiation that is evaluated using standard enclosure method [8]. Details are available elsewhere [7]. The final expressions alone are given below based on the elemental areas shown in Fig. 4. It is to be noted that these same elements are used in solving equation (1) by finite differences.

$$G_i = F_{i-\infty}\sigma T_\infty^4 + \sum_{j=1}^{n_x} F_{i-j}[\varepsilon_b \sigma T_b^4 + (1-\varepsilon_b)G_j] \qquad (2)$$

$$G_j = F_{j-\infty}\sigma T_\infty^4 + \sum_{i=1}^{n_x} F_{j-i}[\varepsilon_f \sigma T_i^4 + (1-\varepsilon_f)G_i]. \qquad (3)$$

The view factors involved in the above expressions are calculated using the contour integral method [9]. The

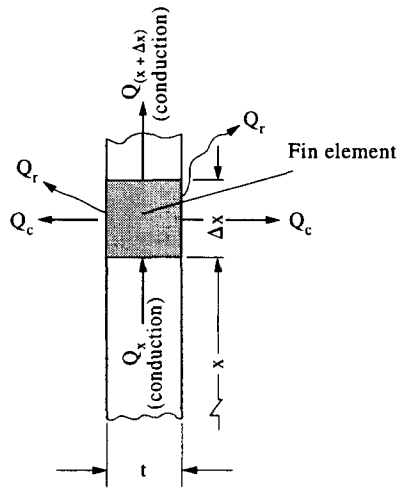

Fig. 3. Schematic showing heat balance for a typical fin element.

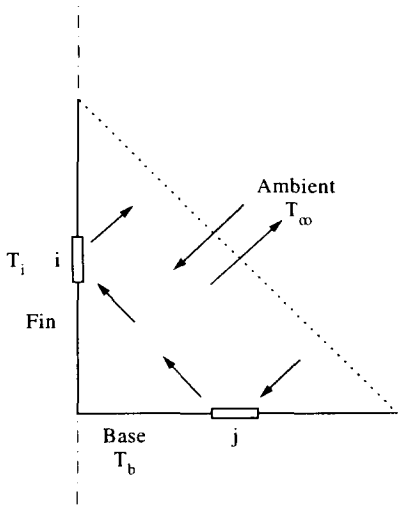

Fig. 4. Sketch showing radiation interaction between the base and fin elements and the ambient. Arrow towards a surface indicates irradiation of the surface. Arrow away from a surface indicates radiosity.

elements are chosen such that the finite difference nodes used in solving the differential equation (equation (1)) fall in the middle of these elements. The radiant flux leaving any of the elements of the fin is then given by the following expression.

$$q_r = \varepsilon_f[\sigma T_i^4 - G_i]. \tag{4}$$

The solutions of the above involve the following stages:

(i) Initialize the temperature to a linear variation between the base and the tip using the measured temperatures.
(ii) Calculate the irradiations using Gauss–Seidel iteration of the simultaneous equations (2) and (3). Repeat the iterations till irradiations converge to the desired level. Since all the temperatures are known (or assumed to start with) these equations are a set of linear equations in the irradiations.
(iii) Revise the temperatures by solving equation (1) by finite difference.
(iv) Repeat steps (ii) and (iii) above till convergence.

The three terms in equation (1) represent, respectively, the conduction, surface convection and surface radiation for an elemental length of the fin. The non-dimensional form of this equation would be

$$\frac{d^2\theta}{d\xi^2} + N_{v\text{-}c} m\theta^2 + N_{r\text{-}c}[\theta^4 - \Gamma] = 0 \tag{5}$$

$$\theta = \frac{T}{T_b}; \quad \xi = \frac{x}{H}; \quad \Gamma = \frac{G}{\sigma T_b^4};$$

$$N_{v\text{-}c} = \frac{2Kk_a H^2 T_b}{k_f t}; \quad N_{r\text{-}c} = \frac{2\sigma\varepsilon_f T_b^3 H^2}{k_f t}. \tag{6}$$

$N_{v\text{-}c}$, the convection conduction parameter can be visualized as a Biot number. However since it appears to depend on the interferometer constant that is dependent on the instrument settings it is advisable to avoid the appearance of K in the non-dimensionalization of the equations. Thus, to present the results the Rayleigh number defined in the usual way is used for describing the free convection heat transfer. The other parameter, $N_{r\text{-}c}$ is the radiation conduction parameter familiar to us in problems that involve an interaction of material conduction and surface radiation.

4. RESULTS AND DISCUSSION

Experiments were conducted for the range of parameters shown in Table 1. The following parameters, however, remained constant at the values shown, in all the experiments: fin thickness $t = 1.5$ mm; fin width $W = 50$ mm; fin thermal conductivity $k = 205$ W m^{-1} K^{-1} (aluminum); base length $B = 50$ mm; base emissivity $\varepsilon_b = 0.85$.

To vary the base temperature the heater input was varied such that the temperature of the base varied in the 320–380 K range. Depending on the ambient temperature (which varied over a small interval during the days on which the experiments were conducted) and the value of the other parameter, the Rayleigh number, was anywhere between 10^4 and 10^7. Throughout this range of Rayleigh numbers the interferograms were steady with no temporal variations which would have signified the presence of turbulent fluctuations. The radiation conduction parameter range was $0.0005 \leqslant N \leqslant 0.1$.

4.1. *Heat transfer characteristics for selected cases*

Some 60 selected experiments in all were conducted as a part of the present study. A few typical tem-

Table 1. Range of parameters used in the present study

Parameter	Range	Remark
Emissivity	0.05, 0.1, 8, 0.47, 0.8, 5	*Obtained by surface preparation/by coating with paints of different colors
Fin height (mm)	30, 50, 70	
Base temperature (K)	320–380	Obtained by using five different heat inputs

* Surface preparation and measurement details are given in ref. [7].

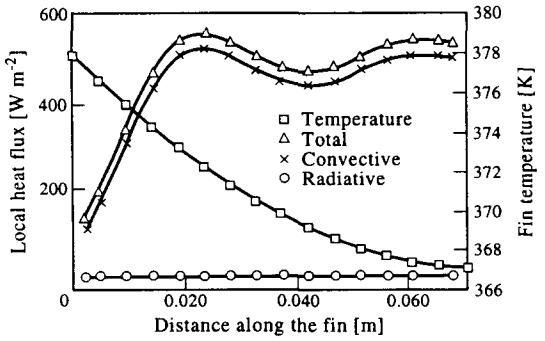

Fig. 5. Variation of local heat fluxes and temperature along the height of the fin: $H = 70$ mm, $\varepsilon_f = 0.05$ (low emissivity case).

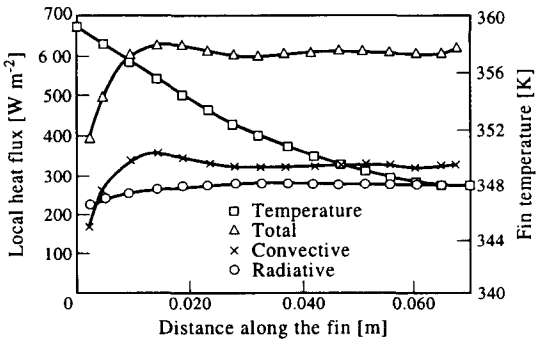

Fig. 6. Variation of local heat fluxes and temperature along the height of the fin: $H = 70$ mm, $\varepsilon_f = 0.85$ (high emissivity case).

perature profile and heat flux profile results are presented in this section. Figure 5 shows the variation with height of the convective, radiative and the total heat flux from the fin surface for the case with $H = 70$ mm, $\varepsilon_f = 0.05$ and $T = 380$ K. The convective heat flux starts with a minimum at the base, reaches a maximum value around $x = 20$ mm. Beyond this there is a gradual decrease in the heat flux with x. For an isothermal vertical flat plate the convective heat flux is infinite at $x = 0$ and then monotonically decreases with x. This is due to the gradual thickening of the boundary layer with x. In the case of the single fin there are two reasons for the observed behavior. First, the fin temperature decreases from the base to the tip and second, the presence of the hot base that causes a heating of the air that flows past it before it encounters the vertically orientated fin. Because of the change in direction of the flow the boundary layer over the vertical surface is affected and, therefore, shows a local minimum and the heat flux a corresponding maximum. Beyond this position the boundary layer grow monotonically and therefore the heat flux shows a gradual decrease. The variation of local convective heat flux is in good agreement with the trends observed by Sobhan *et al.* [6]. The radiative heat flux, however, shows a monotonic increase from the base as we go towards the tip. This behaviour is explained by a monotonic decrease with x of the irradiation of the fin flat by the hot base. Also the view factor from an element on the fin surface to the ambient increases as the element position is changed from near the base to a position near the tip. Figure 6 gives the temperature and heat flux variations for the case of a fin flat with $\varepsilon_f = 0.85$ while all the other parameters are held fixed at the same values as with Fig. 5. The radiative flux starts with a small value near the base and increases steadily as we approach the tip. The variations in the convective and radiative heat fluxes, however, are not reflected in the fin temperature variations. This is a consequence of the large thermal conductivity of the fin material.

4.2. *Contribution of radiation to total heat transfer*

In this section we consider the apportioning of the total heat transfer between the convective and radiative parts. Since the primary objective here is to study the effect of radiation it is instructive to look at the percentage contribution of radiation to the total heat loss. Table 2 shows the results for some representative cases. It is seen that the radiative heat loss varies between some 5 and 50% of the total heat loss. The table shows the results averaged over the five temperature levels achieved in the experiments. The tabulated values show the fin flat contribution alone and therefore do not show the contribution due to the base.

If the fins were assumed to be isothermal it was found that the radiative heat loss would be overestimated by up to about 20% depending on the values of the pertinent parameters. Allowing for a maximum contribution of some 50% due to radiation to the total heat loss, this translates to some 10% to the total heat loss. A similar exercise for convection is not possible since the convective fluxes are a consequence of direct measurement. The interaction between convection and radiation is complex and normally reduces the convective heat loss [10]. However, the reduction in convective heat loss due to radiative interaction was marginal because of the high fin material conductivity. The experimental conditions are such as to make the interaction between conduction and free convection more important than that between radiation and free convection. The temperature distribution in the fin is thus largely governed by this interaction. However, the temperature variation along the fin affects the amount of heat loss by radiation as indicated earlier.

Table 2. Contribution of radiation to total heat transfer in percent

ε_f	$H = 0.03$ m	$H = 0.05$ m	$H = 0.07$ m
0.05	4.9	5.2	5.3
0.18	15.4	16.1	16.6
0.47	31.9	33.2	34.0
0.85	45.8	47.2	48.1

4.3. *Correlations*

Based on the experimental results two correlations have been developed, one for the total heat transfer and another for the radiative loss alone.

4.3.1. *Total heat transfer.*

$$Nu_t = 0.287(1+N_{r-c})^{2.816} Ra_H^{0.277}(1+\varepsilon_f)^{0.866} \quad (7)$$

with a correlation coefficient = 0.983, standard error = 0.032.

4.3.2. *Radiative heat transfer.*

$$Nu_r = 660 N_{r-c}^{0.724} Ra_H^{-0.143} \varepsilon_f^{0.264} \quad (8)$$

with a correlation coefficient = 0.999, standard error = 0.0092.

Correlation for the total Nusselt number is chosen in the above form so that it reduces to the pure convection case when $\varepsilon_f = 0$. Indeed, it reduces to $Nu_c = 0.287\ Ra_H^{0.277}$, which is a common form for free convection heat transfer. This may be compared with the expression $Nu_c = 0.347\ Ra_H^{0.280}$ obtained in [4] by Ruiz and Sparrow for the two legs of the L-corner maintained under isothermal conditions. The exponents in the two formulae agree very closely. However, as expected, temperature variation along the vertical leg, in the present case, tends to reduce the Nusselt number. The role of the height was explicitly brought out through the Rayleigh number based on height apart from its presence in the radiation conduction interaction parameter. The appearance of the Rayleigh number in the correlation for radiative Nusselt number shows a mild interaction between radiation and free convection. The power of ε_f in equation (8) is $0.724+0.264 = 0.988$, a near linear dependence. For a vertical flat plate the index will be exactly equal to unity. The slight departure from unity in the present case is due to radiative interaction with the base and also the temperature variation along the fin. Since the values of N_{r-c} are low the constant 660 appearing in the equation is very large. A detailed error analysis presented in ref. [7] showed that the total uncertainty in Nu_t was between 1.5 and 2.5% while that for Nu_r was between 3 and 30%. The highest uncertainty of 30% occurred for the lowest emissivity cases with $\varepsilon_f = 0.05$. Since the radiation contribution is only about 5% for these cases this translates to an uncertainty of about 1.5% in total heat transfer.

Figures 7 and 8 show parity plots concerning the two correlations given, respectively, by equations (7) and (8). These plots also indicate $\pm 10\%$ error bands, indicating the quality of the two correlations that have been evolved.

5. COMPARISONS WITH A NUMERICAL SOLUTION

Balaji and Venkateshan [5] have solved the problem of combined free convection, conduction and radiation in the case of an L shaped corner. This geometry is similar to the single fin considered in the present study, under the assumption of two-dimensional flow and temperature fields in the flowing medium. A finite volume method was used to solve the governing equations written in the vorticity stream function formulation. Radiosity and irradiations were assumed to vary only along the height and across the base. In the experiments the radiosities and irradiations varied along the width direction also. Therefore the comparisons may be taken only as qualitative. Typically at $Ra_H = 10^6$, $T_b = 380$ K, $T_\infty = 303$ K, equations (7) and (8) predict $Nu_t = 14.16$ and $Nu_r = 1.48$ for $\varepsilon_f = 0.05$. Therefore the experimental value of convective Nusselt number is 12.68 ($= 14.16 - 1.48$). The two-dimensional calculations predict a value of 11.66 for the convective Nusselt number. So, even at a considerably low value of depth to width ratio (unity in the present study) where one would normally expect three-dimensional effects, a two-dimensional approximation yields a satisfactory result. Also, as expected, the numerical result predicts a smaller value for the Nusselt number. This is due to the heat transfer from

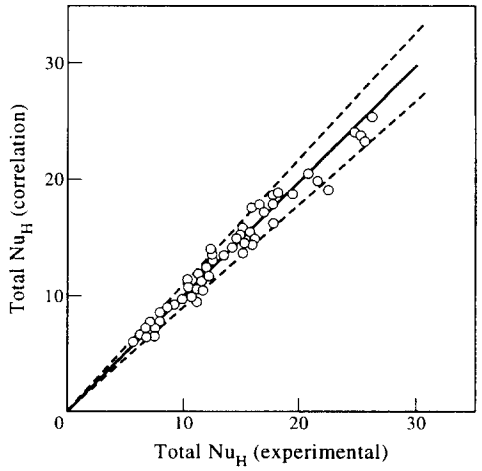

Fig. 7. Parity plot comparing the total Nusselt number from experiments with those from the correlation.

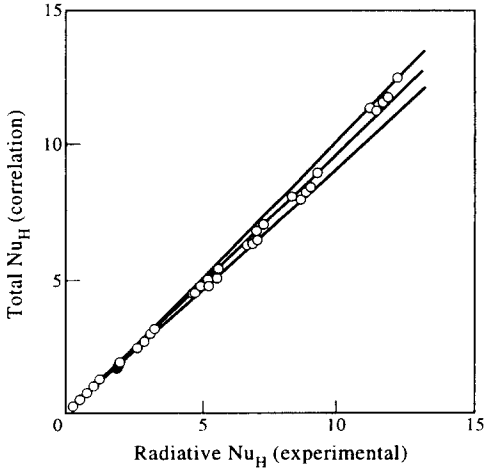

Fig. 8. Parity plot comparing the radiative Nusselt number from experiments with those from the correlation.

the ends, which the two-dimensional calculation does not take into account.

6. CONCLUSIONS

An experimental investigation of free convection and radiation from a single fin has been carried out using a differential interferometer. The radiative part was computed by combining the experimental data with numerical computation based on finite differences. Radiation contribution to total heat transfer has been found to be between 5 and 50% depending on the emissivity and the other parameters. The local convective flux shows a characteristic peak at around 20 mm from the base. This was found to be so for all the fin heights considered in the present study. Correlations have been presented separately for the radiative Nusselt number and the total Nusselt number. Experimental results have been compared with results from a recent numerical study. The qualitative agreement between the two is found to be satisfactory.

REFERENCES

1. Van Leeuwan, J. H., Looman, C. and Schenk, J., Experimental study of velocity and temperature distributions for free convection in a corner. *International Journal of Heat and Mass Transfer*, 1971, **14**, 561–564.
2. Rodigheiro, C. and de Socio, L. M., Some aspects of natural convection in a corner. *ASME Journal of Heat Transfer*, 1983, **105**, 212–214.
3. Angirasa, D. and Mahajan, R. L., Natural convection from L shaped corners with adiabatic and cold isothermal walls. *ASME Journal of Heat Transfer*, 1993, **116**, 149–157.
4. Ruiz, R. and Sparrow, E. M., Natural convection in V-shaped and L-shaped corners. *International Journal of Heat and Mass Transfer*, 1987, **30**, 2539–2548.
5. Balaji, C. and Venkateshan, S. P., Natural convection in L-corners with surface radiation and conduction. *ASME Journal of Heat Transfer*, 1996, **118**, 222–225.
6. Sobhan, C. B., Venkateshan, S. P. and Seetharamu, K. N., Experimental studies on steady free convection heat transfer from fins and fin arrays. *Warme und Stoffubertragung*, 1990, **25**, 345–352.
7. Rammohan Rao, V., Interferometric study of interaction between radiation and free convection in fins and fin arrays. Ph.D. thesis, Department of Mechanical Engineering, Indian Institute of Technology, Madras, India, 1992.
8. Hottel, H. C. and Sarofim, A. F., *Radiative Heat Transfer*. McGraw Hill, New York, 1967.
9. Sparrow, E. M. and Cess, R. D., *Radiation Heat Transfer*, Brooks and Cole, Belmont, CA, 1981.
10. Balaji, C., Laminar free convection with conduction and surface radiation in open and closed cavities. Ph.D. thesis, Department of Mechanical Engineering, Indian Institute of Technology, Madras, India, 1994.